AD-A059 919 ROCKWELL INTERNATIONAL LOS ANGELES CA F/G 13/13
THERMONUCLEAR EFFECTS ON SANDWICH-TYPE STRUCTURES.(U)
DEC 77 C SPARLING, J SCHIBLER DNA001-77-C-0092
UNCLASSIFIED DNA-4496F-2 NL

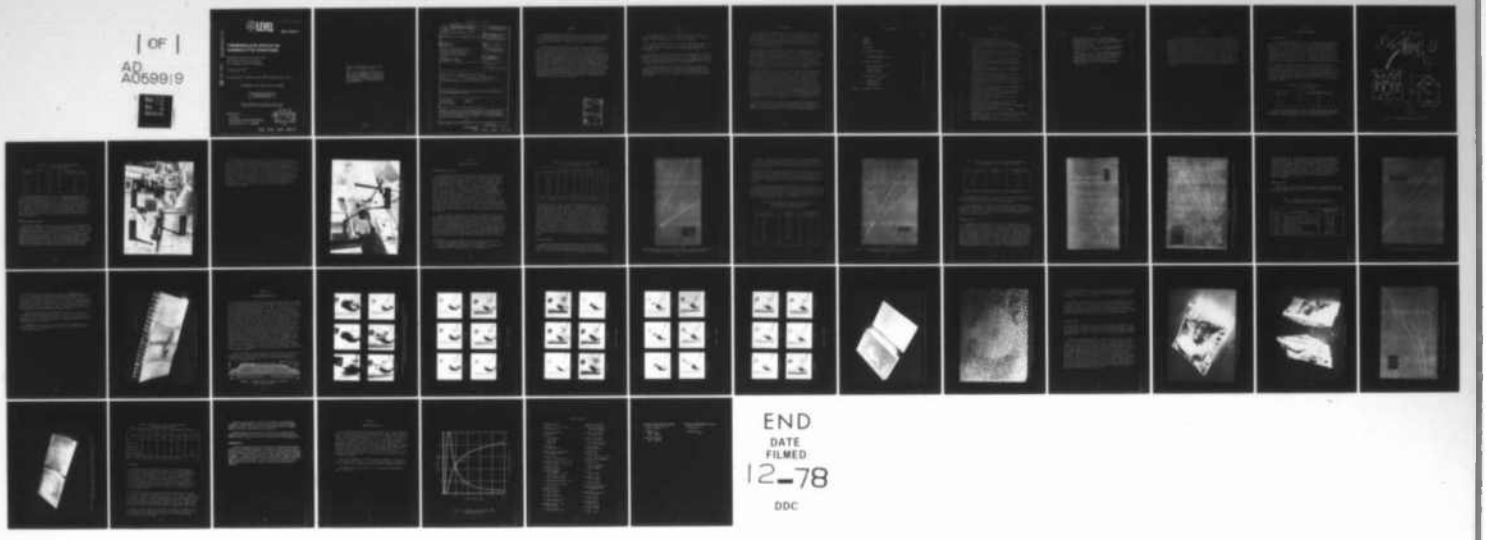

END
DATE FILMED
12-78
DDC

(12) LEVEL II

NW

DNA 4496F-2

THERMONUCLEAR EFFECTS ON SANDWICH-TYPE STRUCTURES

Rockwell International Corporation
5701 West Imperial Highway
Los Angeles, California 90009

1 December 1977

Final Report for Period 1 April 1977—30 November 1977

CONTRACT No. DNA 001-77-C-0092

APPROVED FOR PUBLIC RELEASE;
DISTRIBUTION UNLIMITED.

THIS WORK SPONSORED BY THE DEFENSE NUCLEAR AGENCY
UNDER RDT&E RMSS CODE B342077464 N99QAXAE50303 H2590D.

Prepared for
Director
DEFENSE NUCLEAR AGENCY
Washington, D. C. 20305

Destroy this report when it is no longer needed. Do not return to sender.

PLEASE NOTIFY THE DEFENSE NUCLEAR AGENCY, ATTN: TISI, WASHINGTON, D.C. 20305, IF YOUR ADDRESS IS INCORRECT, IF YOU WISH TO BE DELETED FROM THE DISTRIBUTION LIST, OR IF THE ADDRESSEE IS NO LONGER EMPLOYED BY YOUR ORGANIZATION.

UNCLASSIFIED

SECURITY CLASSIFICATION OF THIS PAGE (When Data Entered)

(18) DNA, SBIE

REPORT DOCUMENTATION PAGE

READ INSTRUCTIONS BEFORE COMPLETING FORM

(4) 1. REPORT NUMBER: DNA 4496F-2 — AD-E 300 339

2. GOVT ACCESSION NO

3. RECIPIENT'S CATALOG NUMBER

(6) 4. TITLE (and Subtitle): THERMONUCLEAR EFFECTS ON SANDWICH-TYPE STRUCTURES

(3) 5. TYPE OF REPORT & PERIOD COVERED: Final Report for Period 1 Apr 77 — 30 Nov 77

6. PERFORMING ORG. REPORT NUMBER

(10) 7. AUTHOR(s): Craig Sparling, John Schibler

(12) 8. CONTRACT OR GRANT NUMBER(s): DNA 001-77-C-0092

9. PERFORMING ORGANIZATION NAME AND ADDRESS
Rockwell International Corporation
5701 West Imperial Highway
Los Angeles, California 90009

10. PROGRAM ELEMENT, PROJECT, TASK AREA & WORK UNIT NUMBERS
Subtask N99QAXAE503-03

11. CONTROLLING OFFICE NAME AND ADDRESS
Director
Defense Nuclear Agency
Washington, D.C. 20305

(11) 12. REPORT DATE: 1 December 1977

13. NUMBER OF PAGES: 46

14. MONITORING AGENCY NAME & ADDRESS (if different from Controlling Office)

15. SECURITY CLASS (of this report): UNCLASSIFIED

15a. DECLASSIFICATION/DOWNGRADING SCHEDULE

16. DISTRIBUTION STATEMENT (of this Report)

Approved for public release; distribution unlimited.

(15) 47 p. (16) N99QAXA (17) E 503

17. DISTRIBUTION STATEMENT (of the abstract entered in Block 20, if different from Report)

18. SUPPLEMENTARY NOTES

This work sponsored by the Defense Nuclear Agency under RDT&E RMSS Code B342077464 N99QAXAE50303 H2590D.

19. KEY WORDS (Continue on reverse side if necessary and identify by block number)

Thermal Pulse
Cell Pressure
Honeycomb Sandwich
Transducer
Humidity

20. ABSTRACT (Continue on reverse side if necessary and identify by block number)

Presence of internal cell pressure during thermal nuclear pulse exposure in honeycomb sandwich structures has been demonstrated. The source of this cell pressure has been shown to be a combination of component outgassing, and the effects of heating a sealed gas (Boyle's law). Cell pressure tests were run at 10 to 50 cal/cm.

DD FORM 1 JAN 73 1473 EDITION OF 1 NOV 65 IS OBSOLETE

UNCLASSIFIED

SECURITY CLASSIFICATION OF THIS PAGE (When Data Entered)

390 899

SUMMARY

The primary objective of Thermonuclear Effects on Sandwich-Type Structures was to develop and validate a method of determining the internal cell pressure in honeycomb sandwich structures during thermonuclear exposure and to perform a test program to determine the magnitude and sources of the internal cell pressure.

The objectives were accomplished by the development and evaluation of various methods for measurement and recording of internal cell pressure. The method selected for the evaluation of cell pressure in typical and field service sandwich panels was the macrotransducer. By utilizing the macrotransducer, thermonuclear-induced cell pressures as high as 20 psi were demonstrated and recorded. Testing indicated that substantially higher cell pressures were present in some test specimens at peak energy levels. However, we were unable to record these transitory pressures due to simultaneous thermally induced catastrophic delamination of the exterior face sheet on these honeycomb sandwich structures. The test phase primarily elucidated the relationship between various adhesives, honeycomb core materials, face sheet materials, and internal cell pressures induced by thermonuclear pulse exposure. These tests demonstrated that the coefficient of thermal conductivity of the face sheet and honeycomb core materials and the outgassing properties of the adhesives are the prime movers in cell pressure increases.

PREFACE

This report describes the investigation conducted to determine the presence, magnitude, and sources of internal cell pressures in honeycomb sandwich structures during thermal nuclear pulse exposure.

This work was funded by the Defense Nuclear Agency under contract DNA 001-77-C-0092. The contract officers were Major David Garrison and Captain Mike Rafferty. The period of performance was from April 1977 to 30 November 1977.

The authors wish to thank Major Garrison and Captain Rafferty for their guidance and support during the performance of this contract. The authors would also like to acknowledge the Air Force Avionics Laboratory (AFAL) and Air Force Materials Laboratory (AFML) for their invaluable discussions and test participation during the course of this contract.

This was a technology study of thermal nuclear flash induced cell pressures in typical aerospace sandwich structures fabricated utilizing modern materials and technology. The generic composites used are typical of sandwich structures on all current and future aircraft, both commercial and military.

BACKGROUND

Due to advances in thermonuclear technology, the utilization of tactical nuclear weapons as a defensive threat against military aircraft is becoming increasingly probable. This, coupled with the existing offensive first strike threat, deems it increasingly important for these aircraft to be hardened against the environments produced by an endoatmospheric thermonuclear explosion. These hardening factors should be considered at all stages of aircraft system design and development.

The state-of-the-art development of nonmetallic materials suitable for primary/secondary structures of future aircraft in advancing rapidly. The use of these materials has been demonstrated on aircraft and missiles. The cost/weight advantages accrued through their use strongly indicates a much broader application in future weapon systems. The design of a successful structural aircraft component requires that the designer has access to all applicable material properties. To build a sound design, he must utilize all building blocks of proper design, mechanical properties, physical properties, and the environmental effects on these mechanical and physical properties.

A honeycomb sandwich structure is a common design tool for light-weight structures on modern aircraft. In spite of its common usage, little design data exists on the macroenvironment which exists within the sealed honeycomb core. The most hostile and degrading environment affecting this cellular macroatmosphere is exposure to intense thermal-nuclear radiation. It was suspected that intense thermo-radiation could result in a synergistic effect of thermally induced adhesive degradation and high internal cell pressures caused by honeycomb core and adhesive outgassing to cause catastrophic honeycomb sandwich delamination. These cell pressures were not a design criterion for any current aircraft due to the lack of true understanding of the problem coupled with a complete lack of design data. During this program, a method of reading and recording these internal pressures was developed and utilized for determining the sources and magnitudes of these internal honeycomb cell pressures.

LAD utilized its unique experience to conduct this 9-month program in support of the Defense Nuclear Agency's investigation of the response of nonmetallic materials when subjected to thermonuclear pulses, simulating those produced from the endoatmospheric detonation of thermonuclear weapons.

TABLE OF CONTENTS

LIST OF ILLUSTRATIONS

LIST OF TABLES

SECTION I

INTRODUCTION

Task I of this program was conducted in an effort to produce experimental data showing the response of selected nonmetallic sandwich materials when exposed to thermonuclear pulses. This necessitated choosing a viable method for testing and recording internal cell pressures. Once this was completed, an evaluation of several of the materials used in honeycomb sandwich construction were performed. Some of these test panels were constructed in the LAD laboratory facility. Other specimens included Air Force-supplied panels, while still others were accelerated weathering panels exposed to 30 days at 96- to 99-percent relative humidity and 170° F. From this testing, an accurate assessment of the source of these pressure buildups can be made. Whether it was caused by the expanding of the heated internal air, the outgassing of the construction materials, or the greater pressures associated with the vaporization of moisture contained within those exposed to moist or humidified atmospheres.

SECTION II

TEST METHOD DEVELOPMENT

STRAIN GAGE METHOD

The first method used to record cell pressure was by utilizing strain gages. A small, linear strain gage with a 0.125 gage length was bonded to the back face sheet of a 0.250 aluminum honeycomb panel. For uniformity, these specimens were 3- by 5-inch rectangles. Placement of the strain gage was directly over a cell, and as close to the middle of the 3- by 5-inch rectangular panel as possible. As the air expands within the cell, tensile stresses should be recorded. The front exposed face sheet was painted with a high-temperature black acrylic paint. During a thermonuclear pulse, the strain in microinches was read off the Doric digital recorder, as shown in Figure 1. Figure 1a shows the equipment used for this test, as well as how it was set up.

The specimens (signal in) were hooked directly to the switching unit P_2 S_2 terminals. The bridge, shown in Figure 1b, plugs into the S+, S-, P-, and P+ terminals, as shown. Also connected to the P+ and P- terminals are the pulse leads from a 1-1/2 volt, dry-cell battery. The other two positions located at the intersection of the bridge and switching unit, labeled S+ and S-, are the signal-out leads routed to the Doric digital recorder. All specimens showed a negative readout when subjected to a 11.1-cal/cm^2 absorbtion pulse (Table 1).

Table 1. Strain in Microstrains at 11.1-cal/cm^2 Absorbed

Specimen	Stable Peak (Microstrains)
1	-71
2	-73
3	-69

A fixture for pressurizing the panel was bonded to the front face sheet of specimen 1. This was to equate strain recorded from the Doric instrument to actual pressures read from a calibrated dial pressure gage (Table 2).

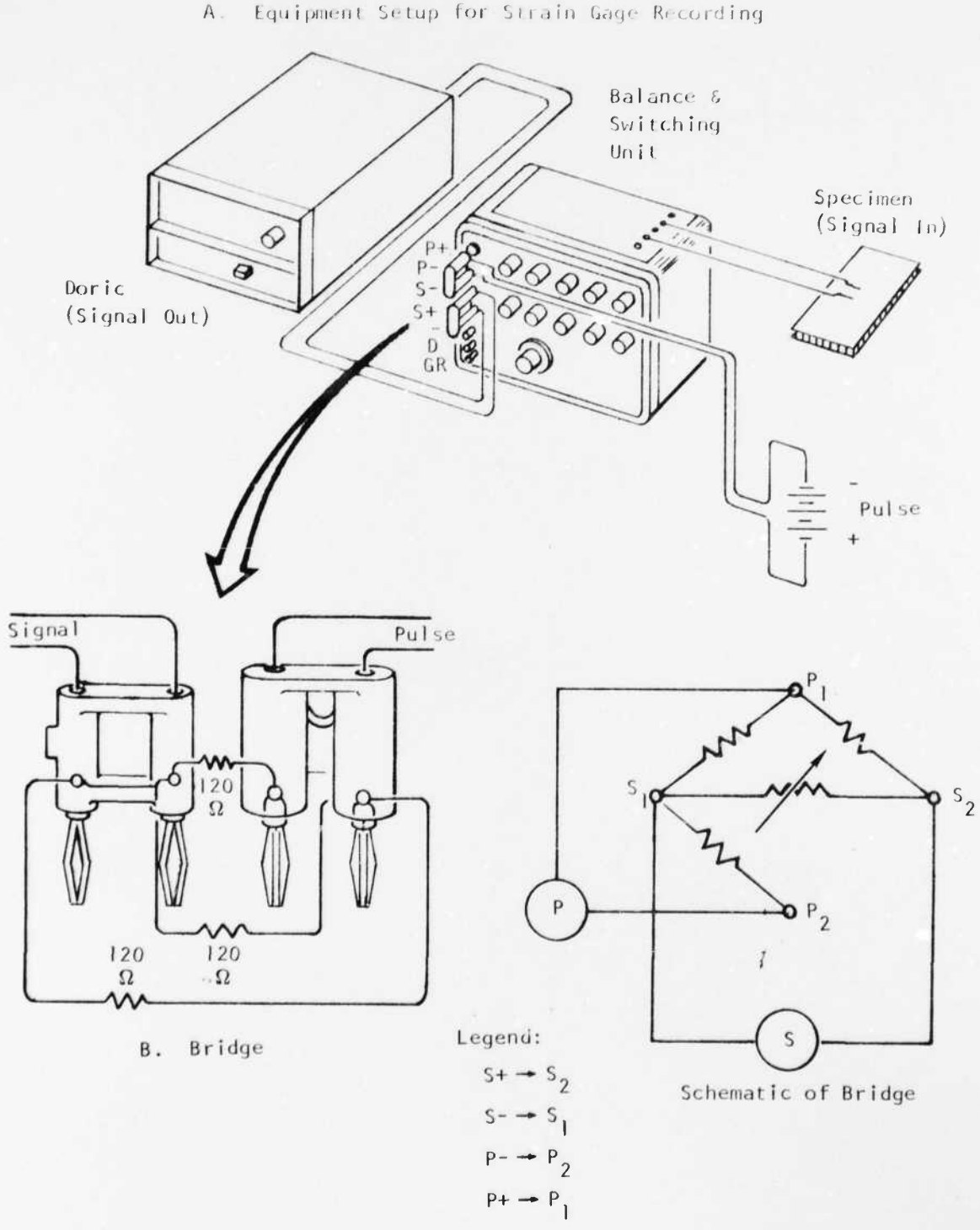

Figure 1. Strain gage equipment used for task 1.

Table 2. Pressurization of Specimen 1 and its Associated Strain

Specimen	psi	Strain (Microstrains)
1	5 (±0.5)	4
	10	12
	20	22
	50	56
	100	102

The result showed that the idea of strain gaging the specimens was not a viable solution for recording cell pressures. The honeycomb panel, when exposed to the thermonuclear pulse, acted as a bending beam. The exposed face sheet heated to much higher temperatures than the back strain-gaged face sheet. The air within the cell expanded but any tension on the rear face sheet was far overpowered by the bending beam action the honeycomb panel went through as the front face sheet went into tension causing the back face sheet to go into compression. This bending beam phenomena, and subsequent compression on the strain-gaged rear face sheet, was recorded as negative values on the Doric instrumentation.

PRESSURE TRANSDUCER METHOD

An alternate method for recording cell pressure utilized an Endevco model 8510-100 pressure transducer. The transducer was energized with 10-volt dc from a regulated dc power supply. A calibrated digital voltmeter was used to establish that the energizing voltage was precisely 10 volts (Figure 2). This transducer responds to a pressure input by generating a dc millivolt output that is proportional to the applied pressure. An x-y strip chart recorder was used to keep a time-versus-millivolt recording of the transducer output. The total apparatus was calibrated by pressurizing both the transducer and a calibrated round-dial pressure gage in a common manifold system. Millivolt readings on the strip chart recorder corresponding to given pressures were determined.

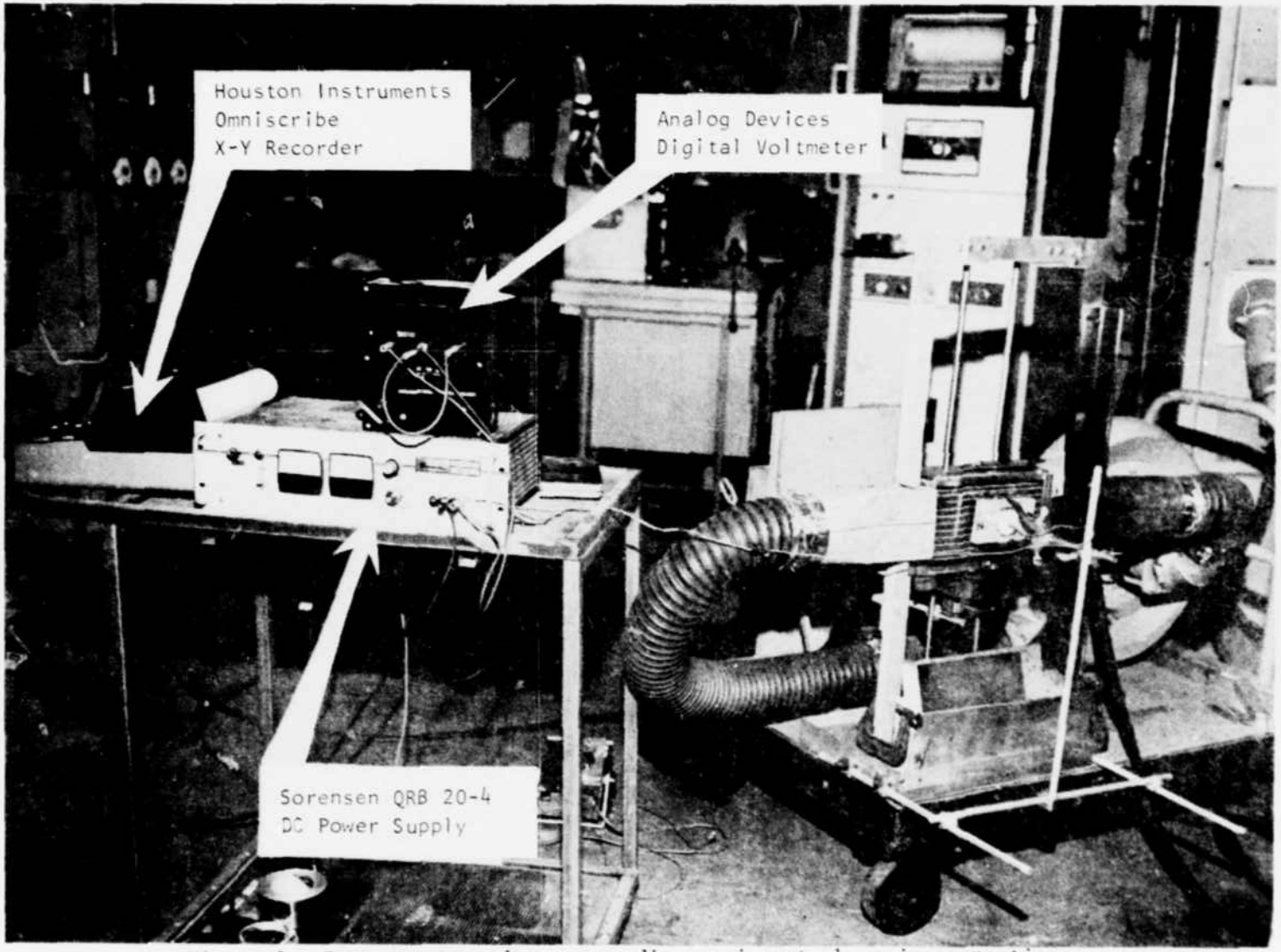

Figure 2. Pressure transducer recording equipment shown in connection with thermonuclear pulse equipment.

The connection of the transducer to the specimen was done using an intermediate aluminum mount (Figure 3). The mounts were tapped to a 10-32 standard screw size, enabling the already threaded transducer to be screwed down, sealing with a rubber O-ring. Several of these aluminum fixtures were machined and bonded to the specimens to be tested directly over a hole drilled in the center of the rear face sheet of the panel. This allowed the transducer to be screwed down into the fixture, leaving the sensor just inside the panel rear face sheet. This allowed the transducer to be interchangeable from one specimen to the next. At higher temperatures, a sealing problem developed, and later model specimens were further sealed with an epoxy resin dam built up around the aluminum fixture. This method gave accurate pressure data, and was, hence, settled upon as the mode to record internal cell pressure buildup for the duration of this program.

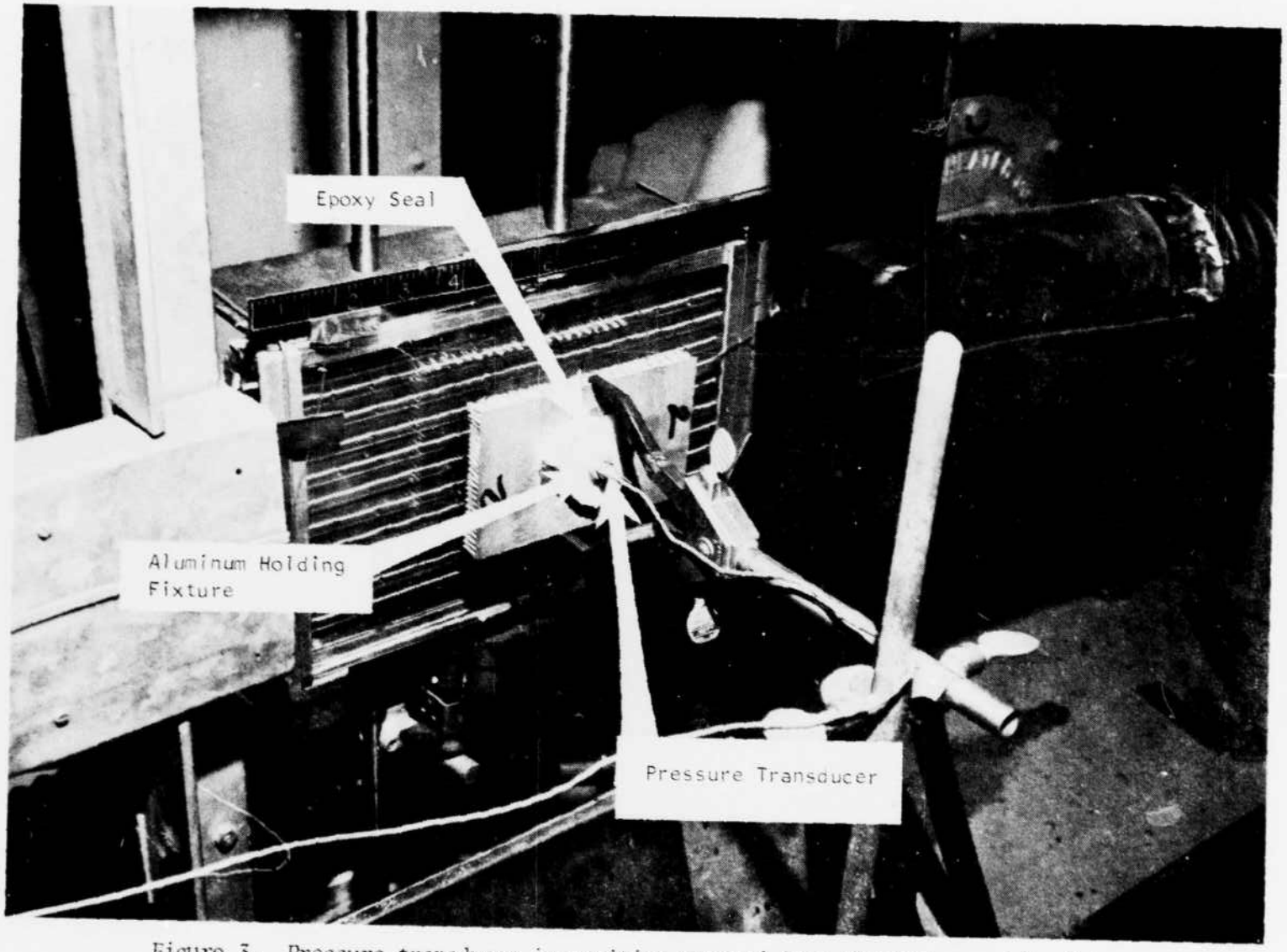

Figure 3. Pressure transducer in position screwed into aluminum mount bonded to rear face sheet of a 3- by 5-inch rectangular test panel.

SECTION III

MATERIALS EVALUATION

HONEYCOMB MATERIAL EFFECTS

Having obtained an accurate means of recording pressure, a material evaluation was performed. The first variable under consideration was the effect the honeycomb material had on the pressures. Four types of core were used, aluminum, HRP, HRH-327, and HRH-10. HRP core is a high-temperature phenolic resin reinforced with a fiberglass cloth. HRH-327 is a polymide resin reinforced with a fiberglass cloth for use at high temperatures for extended periods of time. HRH-10 is a nylon fiber sheet reinforced with phenolic resin. This type of core is for use under a 250° F service temperature. The plastic core-type materials, previously discussed, were sealed around the edges with a polysulfide sealant.(1) This was to prevent the gasses within the honeycomb core from permeating out through the sides of the cell walls. All other aspects of these panels were equal. Their face sheets were 0.025-inch-thick aluminum, and the adhesive was PL-731. PL-731 is an aluminum-filled, modified epoxy adhesive film system with a working temperature range of -67° to 350° F, with a peak pulse range to 420° F. Table 3 shows the results. The values are averaged from three or more pulses at each level. Figure 4 is a representation of these data using the least-squares determination for plotting the lines.(2)

Figure 4 distinctly shows higher pressures associated with panels made from aluminum honeycomb core material over the other nonmetallic cores tested. The points denoting the HRP core material ordinarily would be too random to plot a linear relationship. This random dispersion of points could be caused by faulty seals between the polysulfide and aluminum face sheets. The first three points for the HRP data are reasonably linear and closely parallel to the pressures seen in the other nonmetallic cores. A linear representation of the HRP data was therefore drawn. The higher pressures shown by the aluminum core over the nonmetallic cores is decisive, and lends evidence to the idea of higher pressures being associated with higher thermal conductivity as seen by

(1)* Mil-S-83430, "Sealing Compound, Integral Fuel Tanks, and Fuel Cells Cavities, Intermittent Use to 360° F, 11 December 1973

(2) Military Standardization Handbook, "Metallic Materials and Elements for Aerospace Vehicle Structures, volume 2," paragraph 9.6.3

Table 3. Average Pressures (psi) of Selected Cores at the Energy Levels Listed

Cal/cm^2 Absorbed	Aluminum Core (psi)	HRP Core (psi)	HRH-327 (psi)	HRH-10 (psi)
11.1	6.0	3.5	3.7	3.7
13.9	9.3	4.7	4.8	4.9
16.7	12.1	6.4	5.5	5.9
19.4	15.4	6.3	6.9	8.2
22.2	15.5	5.8	7.4	8.8
25	-	5.4	7.9	-
NOTE: - denotes levels where specimens failed to hold pressure				

the ideal gas law, $pV = nRT$. Another solution would include the porocity of the nonmetallic honeycomb materials. The temperature of the cells around the periphery of the 3- by 5-inch panels would be slightly lower because the edges of the panels extend to the outer edges of the thermonuclear light array where slightly less energy is being absorbed. Whereas, the aluminum core is sealed around each individual cell; the nonmetallic cores are sealed only at the outside edges of the panels. This would allow the pressures in these nonmetallic cores to diffuse evenly over the entire 3- by 5-inch panel before the transducer could record the instantaneous pressure existing within the single cell housing the sensor. This temperature difference experienced within the array is so small that it is not believed to be the cause of our pressure differences. It was taken into consideration to use only aluminum core for the duration of the tests and eliminate nonmetallic honeycomb core materials as a major contributor to cell pressure buildup upon exposure to thermonuclear pulses.

FACE SHEET EFFECTS

To pursue the materials evaluation further, face sheets were the next variable to consider in honeycomb panel construction. The face sheets used for this test were aluminum, graphite/epoxy, and glass-fabric, reinforced epoxy. For the LAD tests, the 0.025-inch-thick aluminum face sheets were used

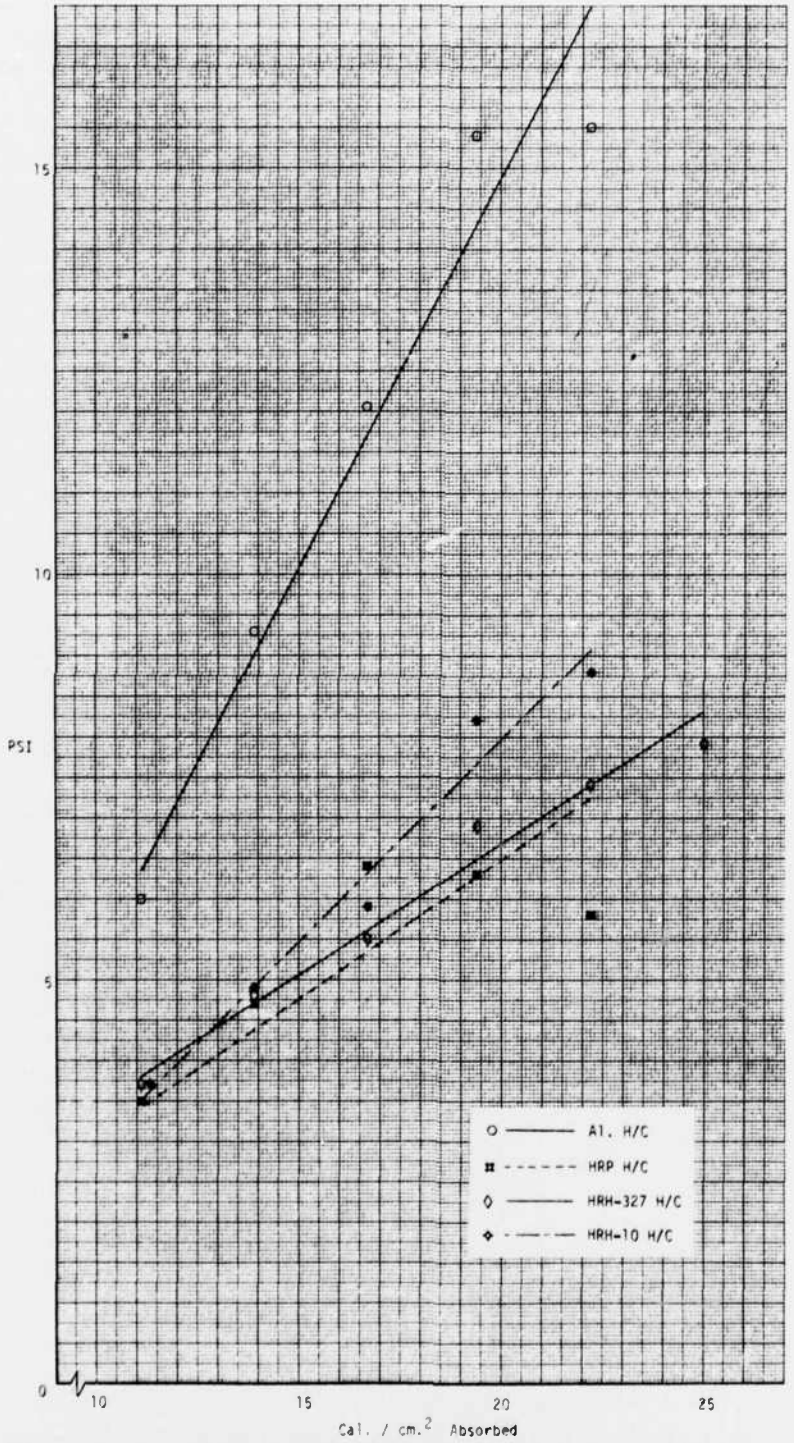

Figure 4. Comparison of honeycomb materials used in sandwich construction as they are effected by increasing energy absorption levels.

as a standard. Table 4 shows a comparison between aluminum and graphite/epoxy face sheets. The graphite/epoxy face sheets were three plies orientated with their fibers [0 45], balanced around the honeycomb core material. Two specimens of each type were constructed and subjected to each pulse for an average of three or more times.

All panels used for this comparison were from 0.825 to 0.925-inch thick, the thicker ones being the graphite/epoxy specimens. The core and adhesive types were both similar for these tests. Figure 5 shows the relationship in Table 4 of aluminum to graphite/epoxy using the least squares determination for plotting the line. These lines cross at 14 cal/cm^2 due to their differences in slope.

Table 5 gives the data for the comparison of glass-fabric reinforced epoxy to aluminum face sheet material. The glass-epoxy face sheets were three-ply orientated with the warp direction all 0-degree in relation with the 5-inch direction of the rectangular panel. All core types used were 0.250-inch thick, and the adhesive was AF-143. AF-143 is a modified epoxy adhesive film system with a working temperature range of -67° to 350° F.

Table 4. Pressure in psi of 0.825 to 0.925-Inch-Thick Honeycomb Sandwiches Made With Aluminum and Graphite-Epoxy Face Sheets

Cal/cm^2 Absorbed	Aluminum (psi	Graphite/Epoxy (psi)
11.1	2.9	1.8
19.4	5.2	
20		5.1
25	7.4	
30	9.7	7.9
35	11.5	
40	16.2	9.2
50		10.9

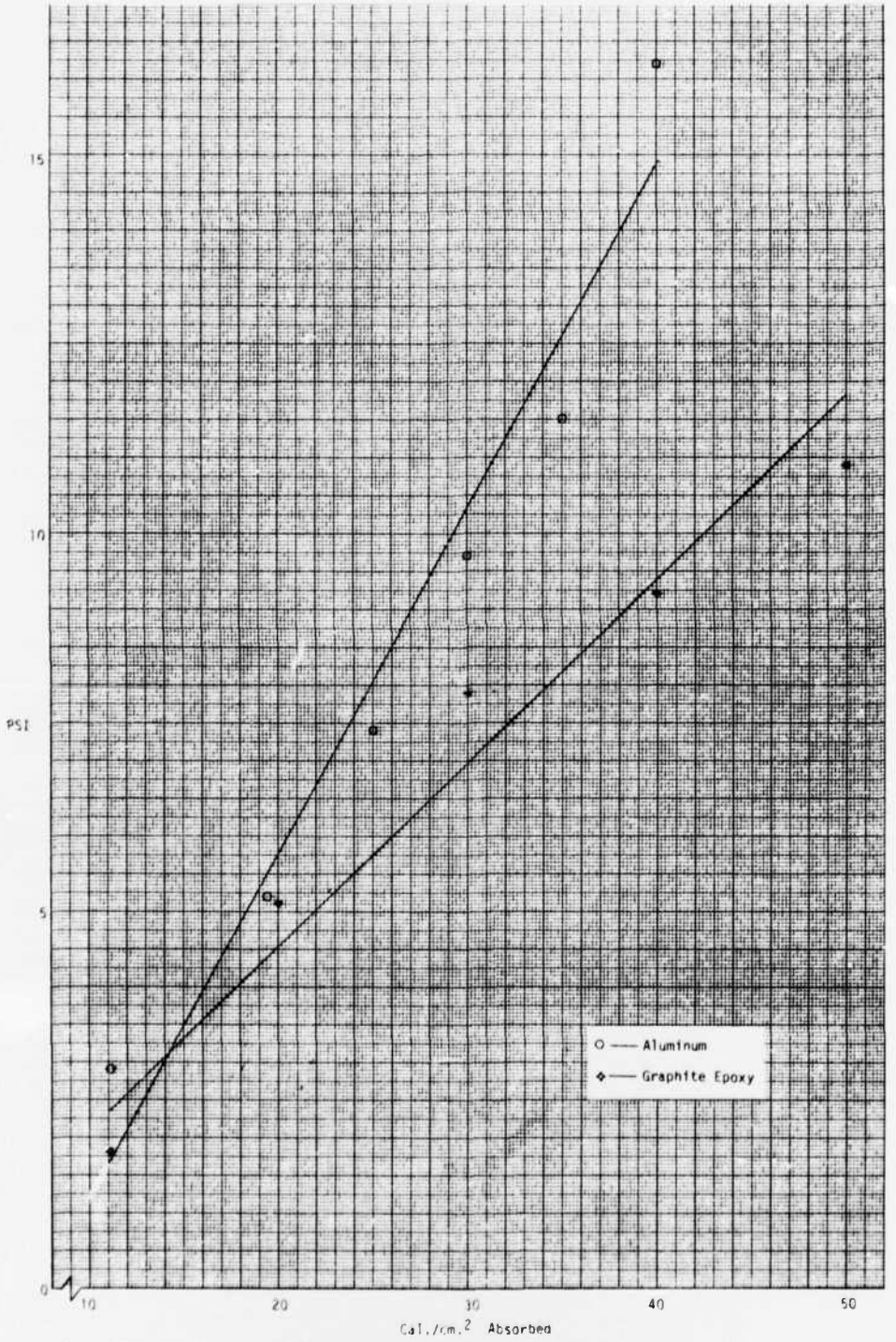

Figure 5. Face sheet effects on pressure increase of aluminum versus graphite/epoxy as energy levels increase.

Table 5. Pressure in psi of 0.025-Inch-Thick Honeycomb Sandwiches with Aluminum and Glass-Fabric Epoxy Face Sheets

Cal/cm^2 Absorbed	Aluminum (psi)	Glass-Fabric Epoxy (psi)
11.1	5.6	3.6
20	7.3	6.1
30	16.3	9.4
40	—	17.4

NOTE: — denotes levels where specimens failed to hold pressure.

Figure 6 shows the results of Table 5 with the lines plotted according to the least squares determination. As was the case in Figure 5, these lines cross at 15 cal/cm^2 again due to their difference in slopes.

In both conditions, the aluminum face sheet panels developed higher pressures over those made of graphite and glass-fabric epoxies. The nonmetallic material face sheets were less affected by thermonuclear pulses, with respect to cell pressures. This is a result of the lower temperatures ensued because of their lower thermal conductivity.

THICKNESS EFFECTS

To pursue this idea of thermal conductivity as a major cause of pressure buildup within the cells, panels were constructed and/or provided by the Air Force, which varied in thickness. Those supplied by the Air Force were from modern tactical aircraft. All the panels were constructed of similar gage aluminum 0.025-to 0.030-inch-thick face sheets and constructed of similar gage aluminum cores. The adhesives used were either AF-130 or AF-143. Both adhesives are modified epoxy adhesive film systems; however, AF-130 has higher strength properties at temperatures up to 400° F. Five different thicknesses were tested. The averages are shown in Figure 7. As the thickness of the honeycomb panel increases, the area within the cells increases. The more volume within the confined intercellular space, the less pressure. This can be explained by the

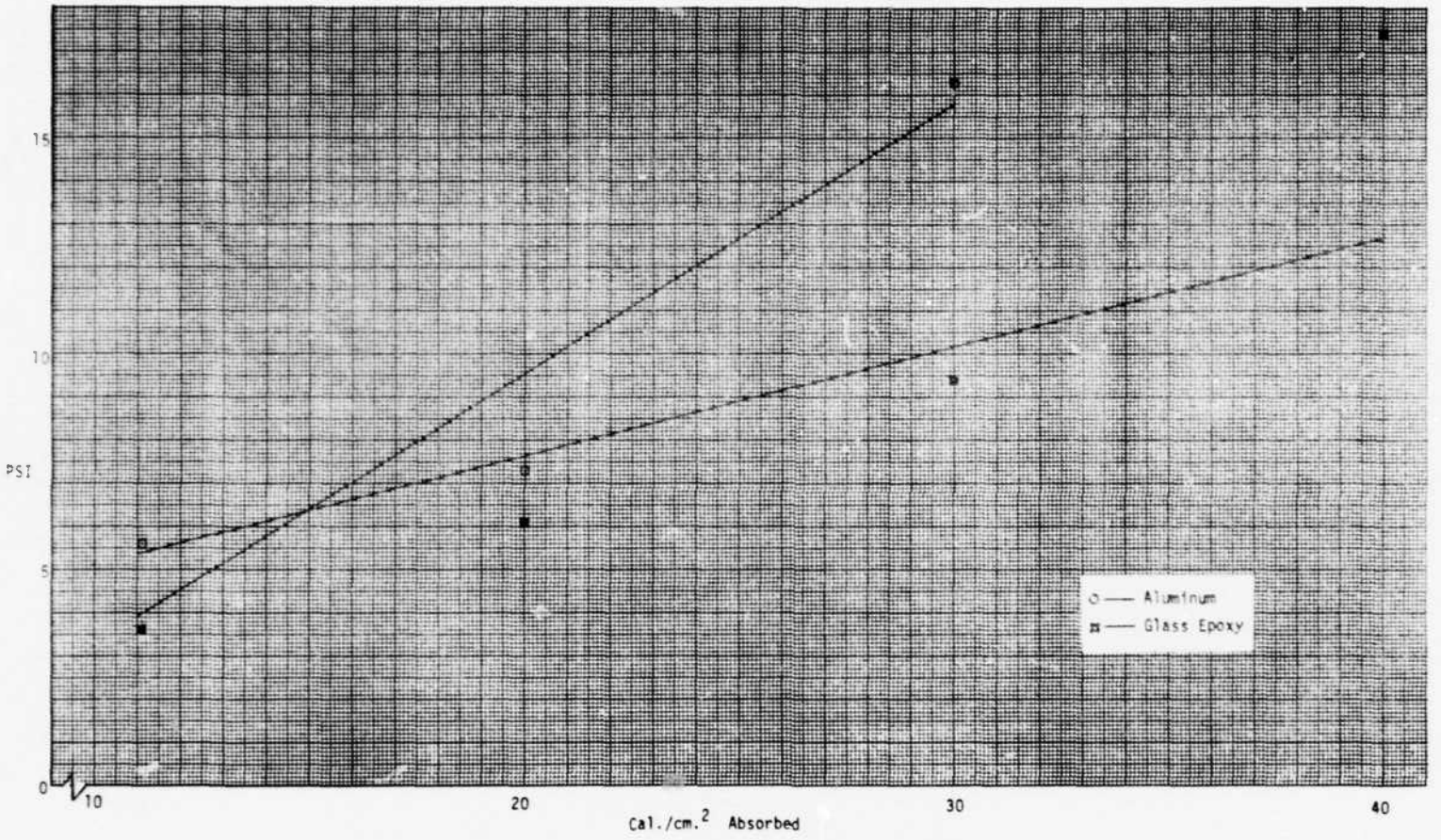

Figure 6. Comparison between aluminum and glass-reinforced epoxy face sheets as they relate to pressure buildup with honeycomb panels.

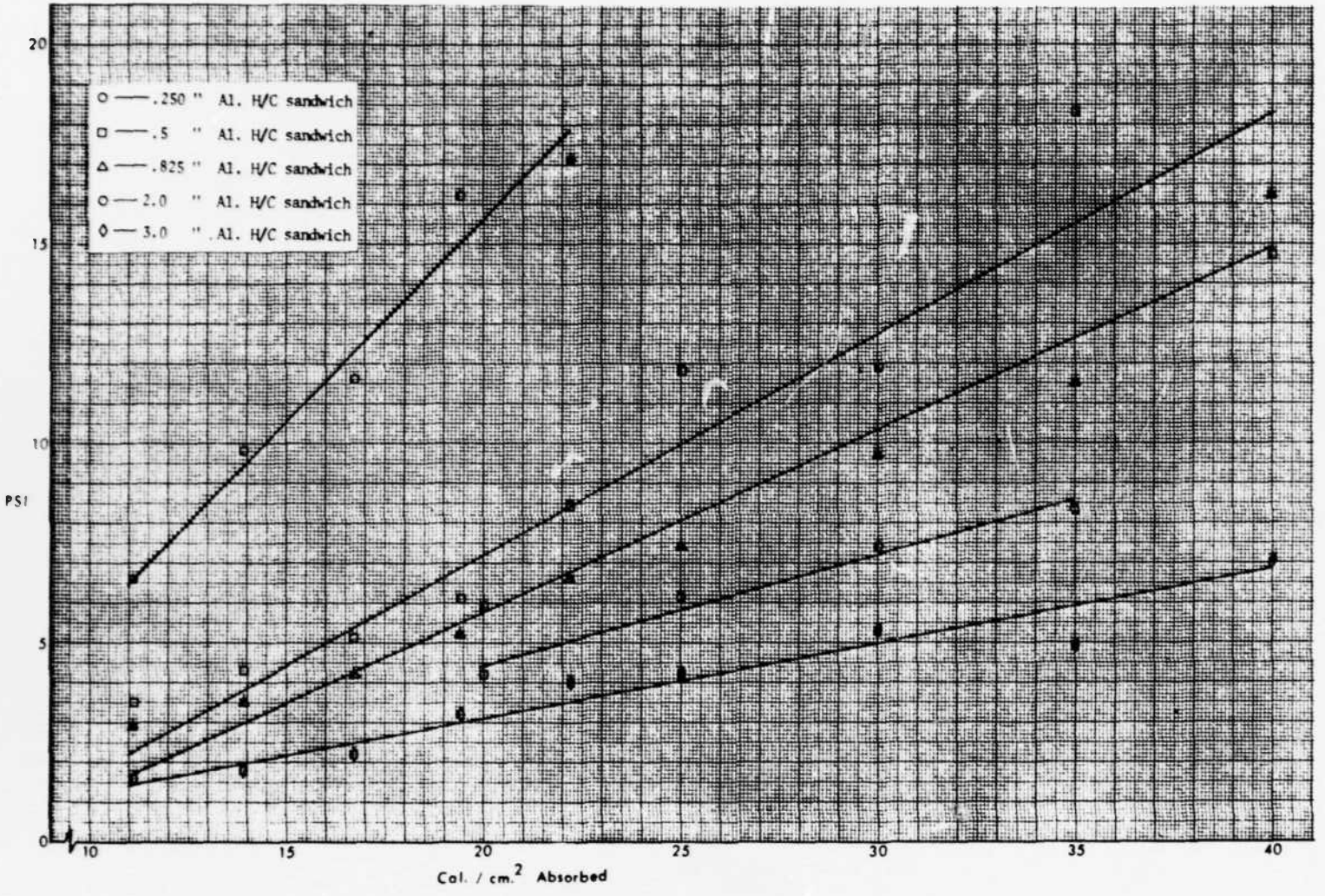

Figure 7. Aluminum honeycomb sandwich panels of varying thicknesses showing pressure within panel increase as energy level increases.

ideal gas law pV = nRT. As the volume increases, the pressure decreases. Along with this, Figure 8 shows the variance in temperatures between the exposed glue line and a point 0.125 inch behind the glue line in the center of the cell. The further away from the exposed surface, the lower are the resultant temperatures. Therefore, not only will the volume affect the equation, but by increasing the distance from the pulse, the temperatures will be less, again lowering the pressure. This evidence lends itself to substantiate that higher pressures are associated with any property of a honeycomb sandwich panel which increases its thermal conductivity (see Figures 4 through 7).

ADHESIVE EFFECTS

The reaction of adhesives to thermonuclear pulses produced varied results. Six adhesive types were evaluated (Table 6) covering working temperature ranges from -423° to 700° F.

Table 6. Adhesive Types and Basic Characteristics for Use in Studying Their Effect on Cell Pressures

Name	General Description	Designed Operating Range (° F)
FM1000	Unsupported polyimide epoxy film	-423 to 200
FM123-5	Modified Nitrile epoxy supported film	-67 to 250
PL 731	Aluminum-filled, modified epoxy film	-67 to 350
AF-143	Modified epoxy film	-67 to 350
AF-130	Modified epoxy film	-67 to 400
FM34B	Polyimide resin on a glass cloth	-400 to 700

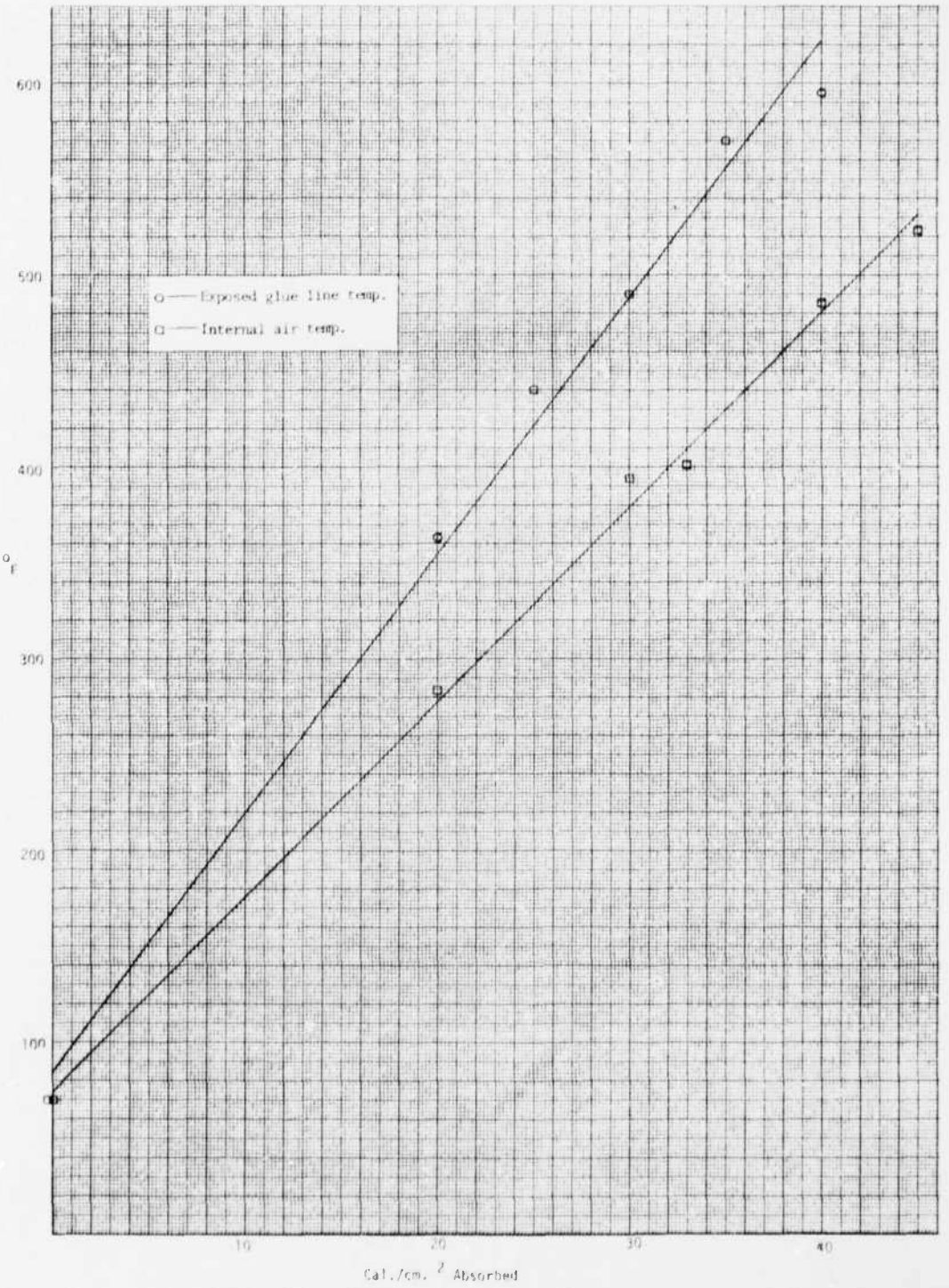

Figure 8. Glue line temperatures as they compare to internal air temperatures with rising energy levels.

Panels that were 0.25-inch thick constructed of aluminum face sheets and core, using the lower temperature range adhesives FM1000 and FM123-5, held pressure resultant from 20 cal/cm^2 absorbed thermonuclear pulses. This was their limit. At higher levels of absorption (25 cal/cm^2), the panels would not hold pressure and small disbonded areas occurred (Figure 9). High-speed motion pictures were taken of a few of these specimens at even higher energy levels. Both at 40 and 35 cal/cm^2, the FM123-5 adhesive completely separated from the honeycomb panel, while the FM1000 panels merely disbonded.

Similar panels made using AF-143 adhesive held pressures up to 35 cal/cm^2 absorbed, and would not totally shed their face sheets even at levels of 50 cal/cm^2. Panels made with PL 731 adhesive reacted similar to AF-143 panels, however they were occasionally untrustworthy in that they leaked pressure out through the nylon scrim carrier.

FM34B adhesive was used on only three panels with no apparent increase due to their use. AF-130 adhesive was the type seen on all the Air Force flight hardware panels tested.

Figure 9. Typical disbond caused from thermonuclear exposure.

SECTION IV

FLIGHT HARDWARE EVALUATION

With regularity, these tactical military aircraft panels made of aluminum core and face sheets would explode with a loud pop accompanied by flames. This type of reaction followed for specimens of thicknesses from 0.25- to 0.825-inch thick at a 40 cal/cm^2 absorbed energy level. These panels held pressure at 30 cal/cm^2 and disbonded slightly at 35 cal/cm^2 absorbed. High-speed motion pictures were taken of this phenomena in an effort to establish if 40 cal/cm^2 absorbed could be the energy level at which the autogenious ignition temperature of the adhesive was reached. Figure 10 shows selected frames from 0.5-inch thick tactical military aircraft being exposed to 40 cal/cm^2 absorbed. At the 1.9-second time interval, gases can be seen evolving from the edges of the front face sheet. The 2.0-second interval starts at 25-frame sequence showing the actual ignition of the escaping gases as the face sheet blows off the panel (2.11 to 2.17 seconds), hits the quartz glass protecting the lamp array (2.18 seconds), and falls to the ground (2.30 seconds). The flame stays in view until the 2.27-second mark for a duration of almost 3/10 second. This clearly shows the ignition of the escaping gases after the face sheet had already disbonded due to the pressure within the cell. The flammable product evolving from the specimen is most probably due to either entrapped volatile solvents or the flash pyrolysis products of the adhesive substrate. The flaming was not a result of AIT. Figure 11 shows the tactical military aircraft and its corresponding face sheet used for the preceding test. Figure 12 shows a closeup of the adhesive on the face sheet to better visualize the extent of the adhesive degradation.

Due to the dramatic results shown by the tactical military aircraft panels and noting that the edges of these panels were the areas the pressure was allowed to escape disbonding the panel, a more representative specimen was constructed (see Figure 13).

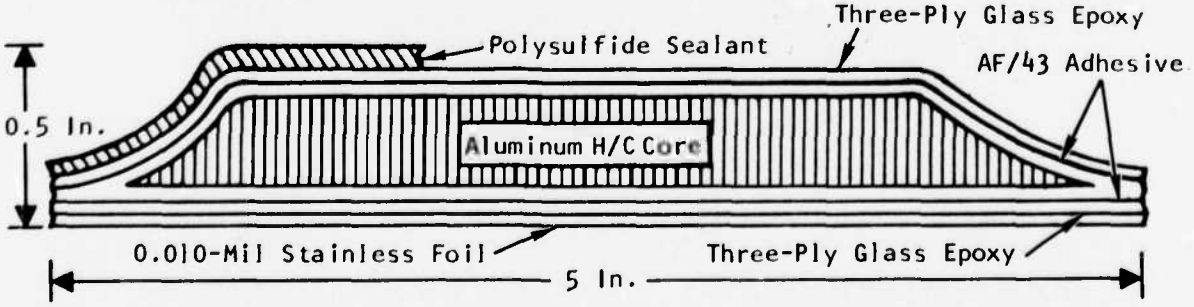

Figure 13. Specimen used to evaluate edge closeout effects on cell pressures.

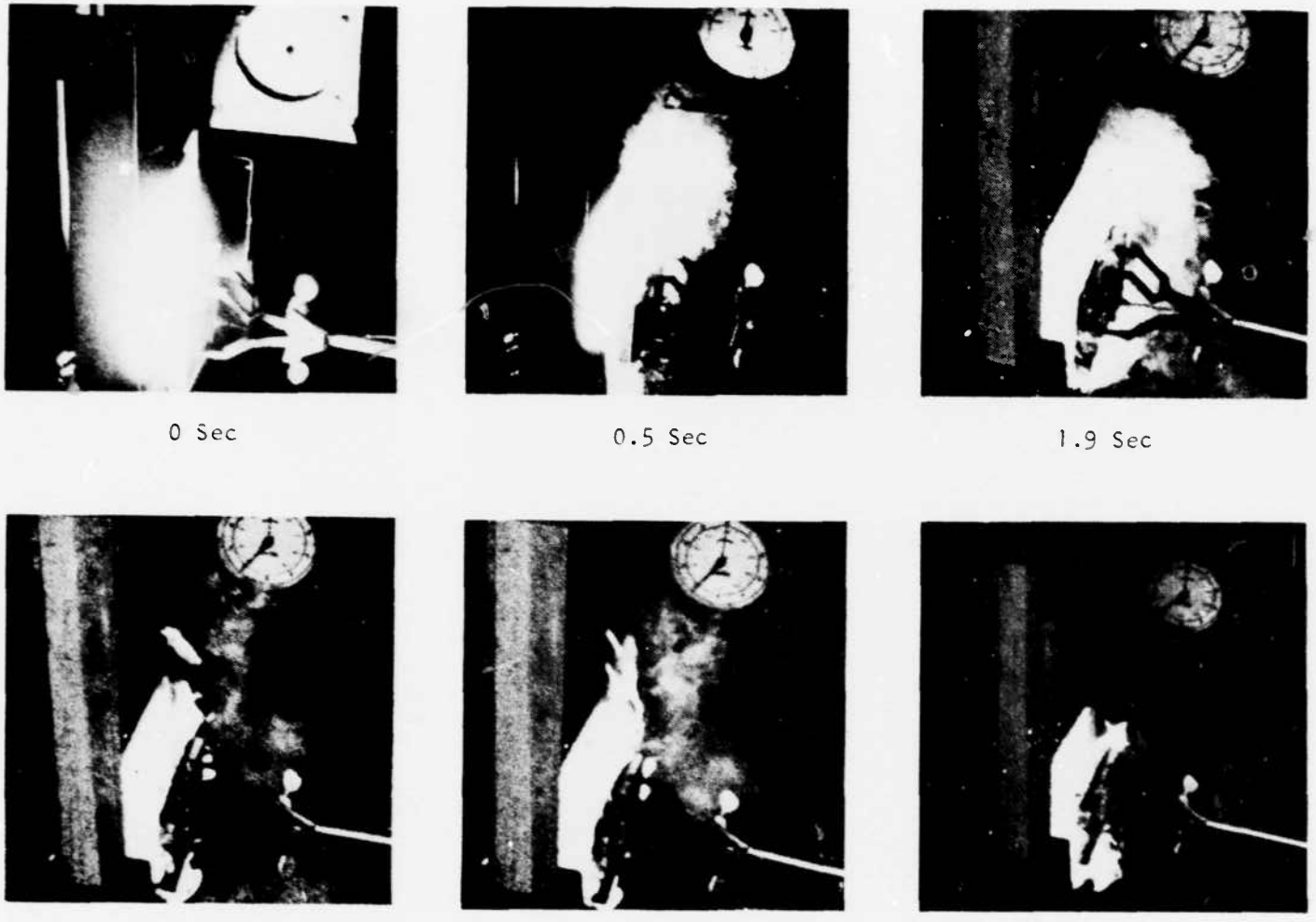

Figure 10. Sequence pictures of an 0.5-inch-thick tactical military aircraft test panel being exposed to a 40 cal/cm^2 absorbed pulse.

2.07 Sec

2.08 Sec

2.09 Sec

2.10 Sec

2.11 Sec

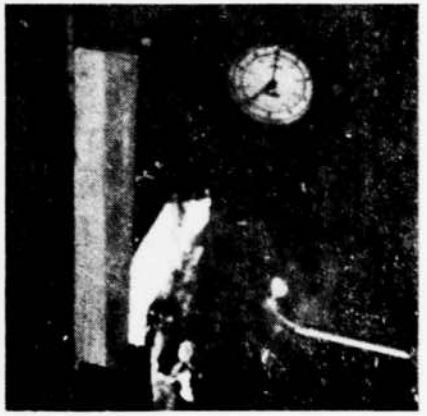

2.12 Sec

Figure 10. Continued.

2.13 Sec

2.14 Sec

2.15 Sec

2.16 Sec

2.17 Sec

2.18 Sec

Figure 10. Continued.

2.19 Sec

2.20 Sec

2.21 Sec

2.22 Sec

2.23 Sec

2.24 Sec

Figure 10. Continued.

2.25 Sec 2.26 Sec 2.27 Sec

2.28 Sec 2.29 Sec 2.30 Sec

Figure 10. Concluded.

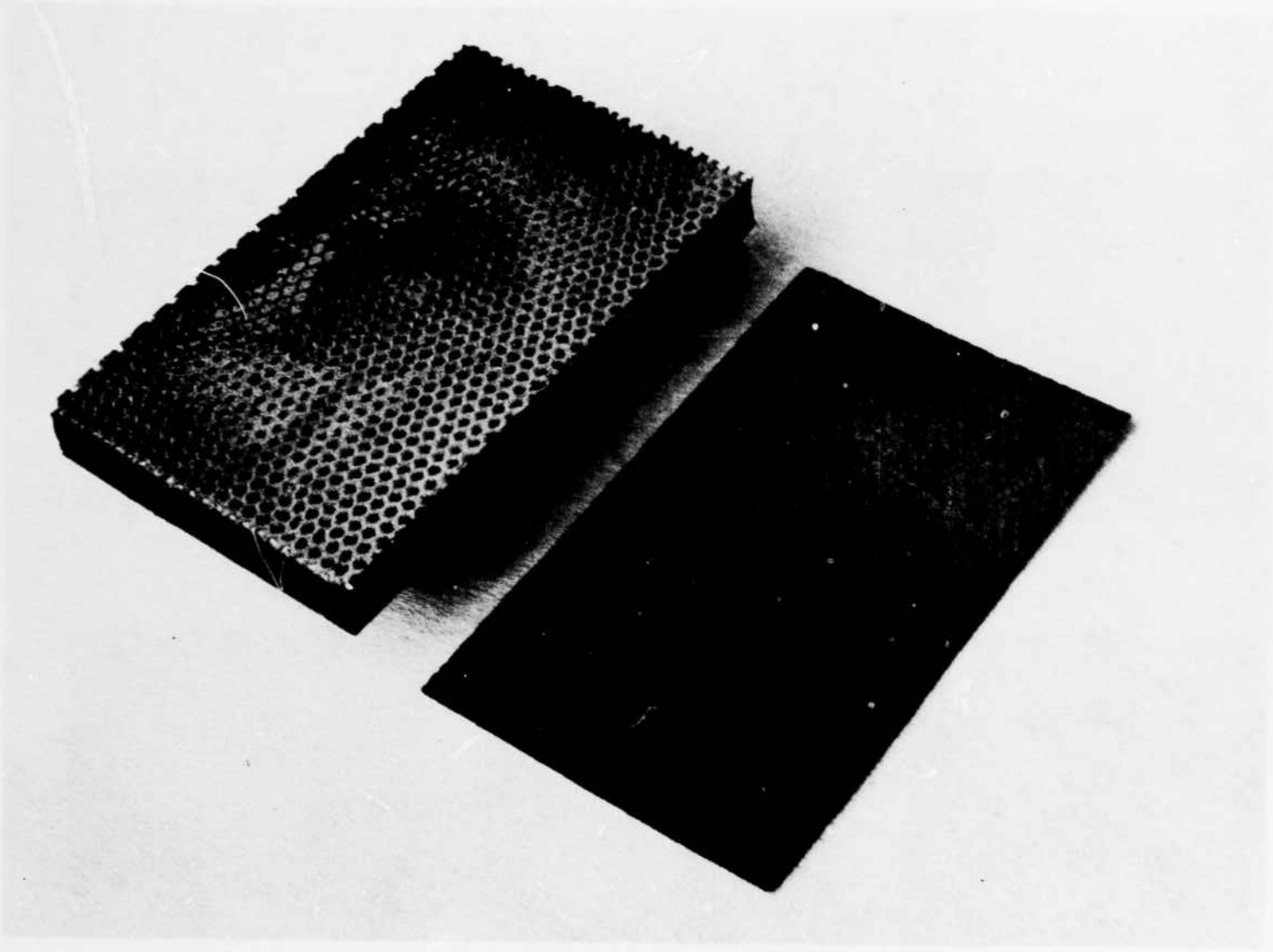

Figure 11. Tactical military aircraft panel following thermonuclear exposure of 40 cal/cm^2 absorbed.

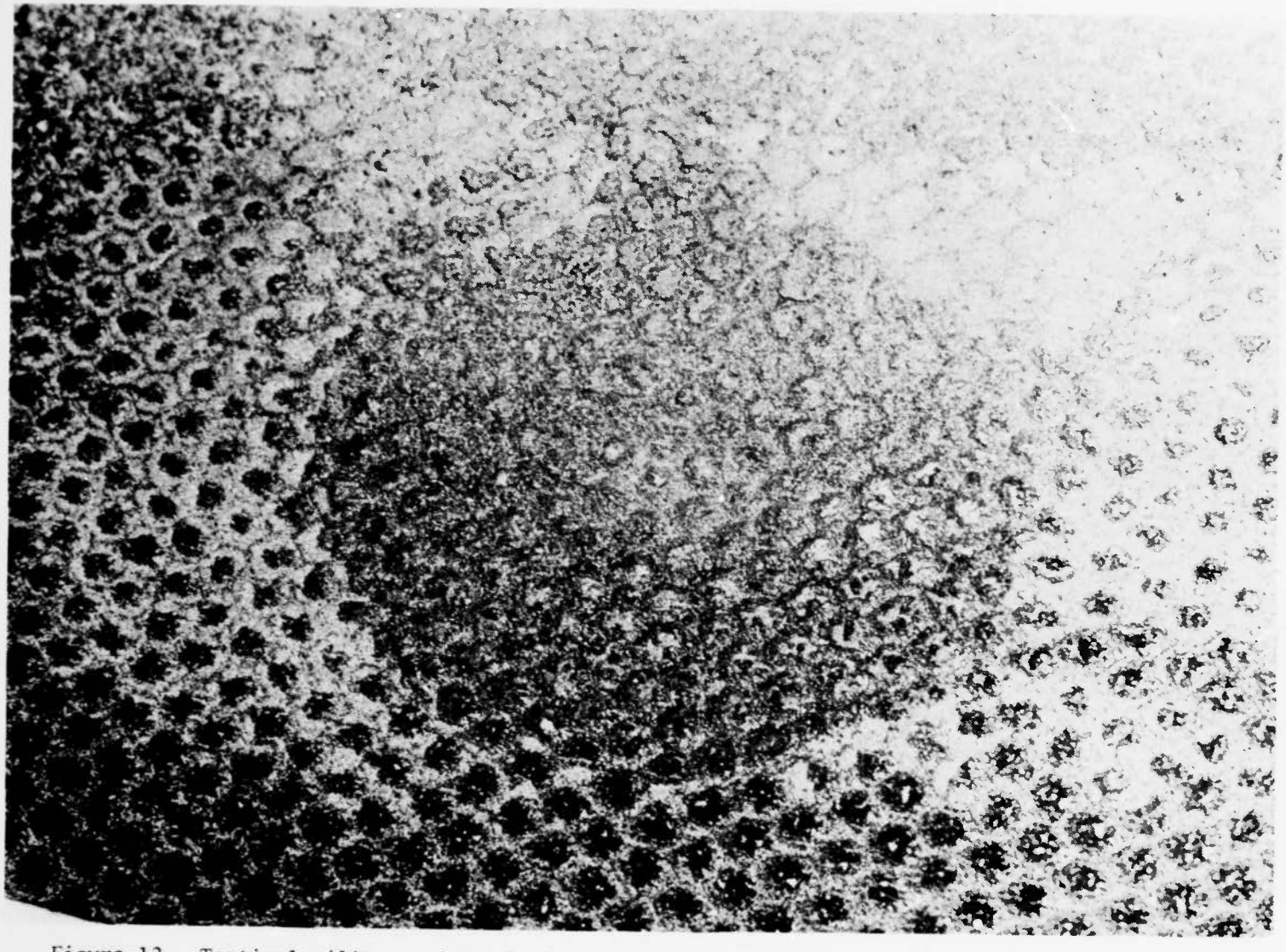

Figure 12. Tactical military aircraft front face sheet showing degradation of adhesive caused by thermonuclear exposure at 40 cal/cm^2 absorbed

Figure 13 is a drawing of a single specimen used to evaluate edge closeout effects on cell pressures. A stainless foil was wrapped around edges of the 5- by 5-inch-square panel, and was sealed to the back of the specimen with polysulfide.

This panel was exposed to a 40-cal/cm^2 absorbed thermonuclear pulse with the results shown in Figure 14. The specimen is shown cut in half to expose the damage in Figure 15. Along with this skin buckling of the stainless secondary face sheet, a 10.2 psi pressure was also recorded. The pressures within the panel were therefore well above the recorded 10.2 psi, as the volume under the buckled face sheet was at least tripled when fully expanded.

HUMIDITY STUDIES

A similar design to Figure 13 was used in studies involving humidity effects on cell pressures. One difference being that the humidity specimens were not encapsuled with a stainless steel shell. Also, they were not made of aluminum honeycomb core but of HRH-10 and HRP cores. The results are shown in Table 7 and Figure 16.

Between each thermonuclear pulse, the humidity panels were subjected to 30 days at 170° F and 96-99% relative humidity. The results show a slight increase in pressure for those panels exposed to humidity conditions. The results also indicate that those panels exposed to humidity might be more resistant to catastrophic failure than their counterpart control panels. The control panels delaminated, causing ply buckling and face sheet splitting at 50 cal/cm^2, while the humidity panels held pressure without any failures (Figure 17). This could be misleading in the overall perspective since those panels were all constructed of nonmetallic glass-reinforced epoxy face sheets. The resin could have become more plasticized due to the moisture and, therefore, more flexible than the resin in the control panels. With metallic face sheets, this explanation would not hold true. The aluminum face sheets would not become plasticized and, therefore, would possible suffer more severe damage caused from moisture within its cells.

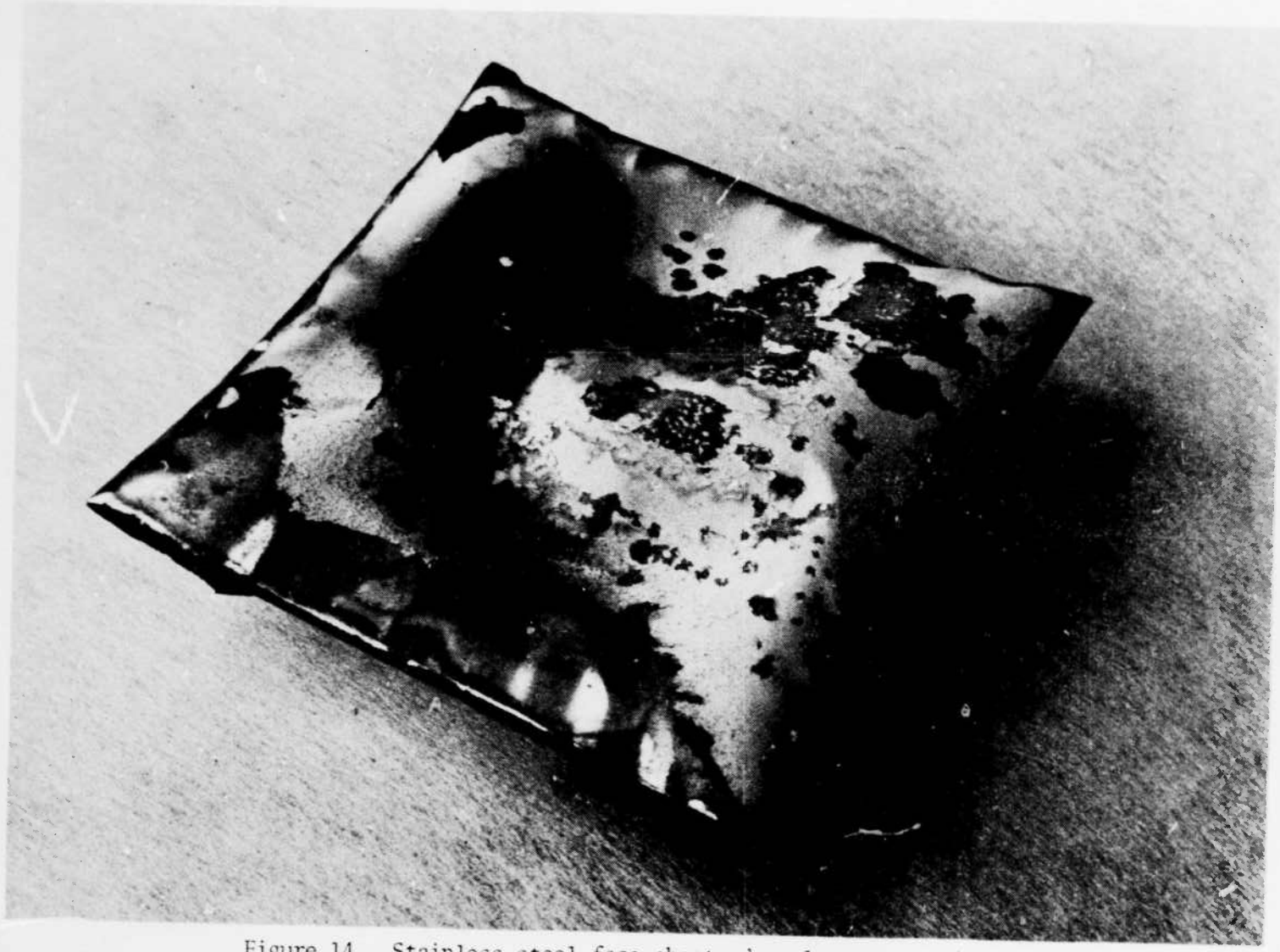

Figure 14. Stainless steel face sheet edge closeout specimen following 40 cal/cm^2 absorbed energy level.

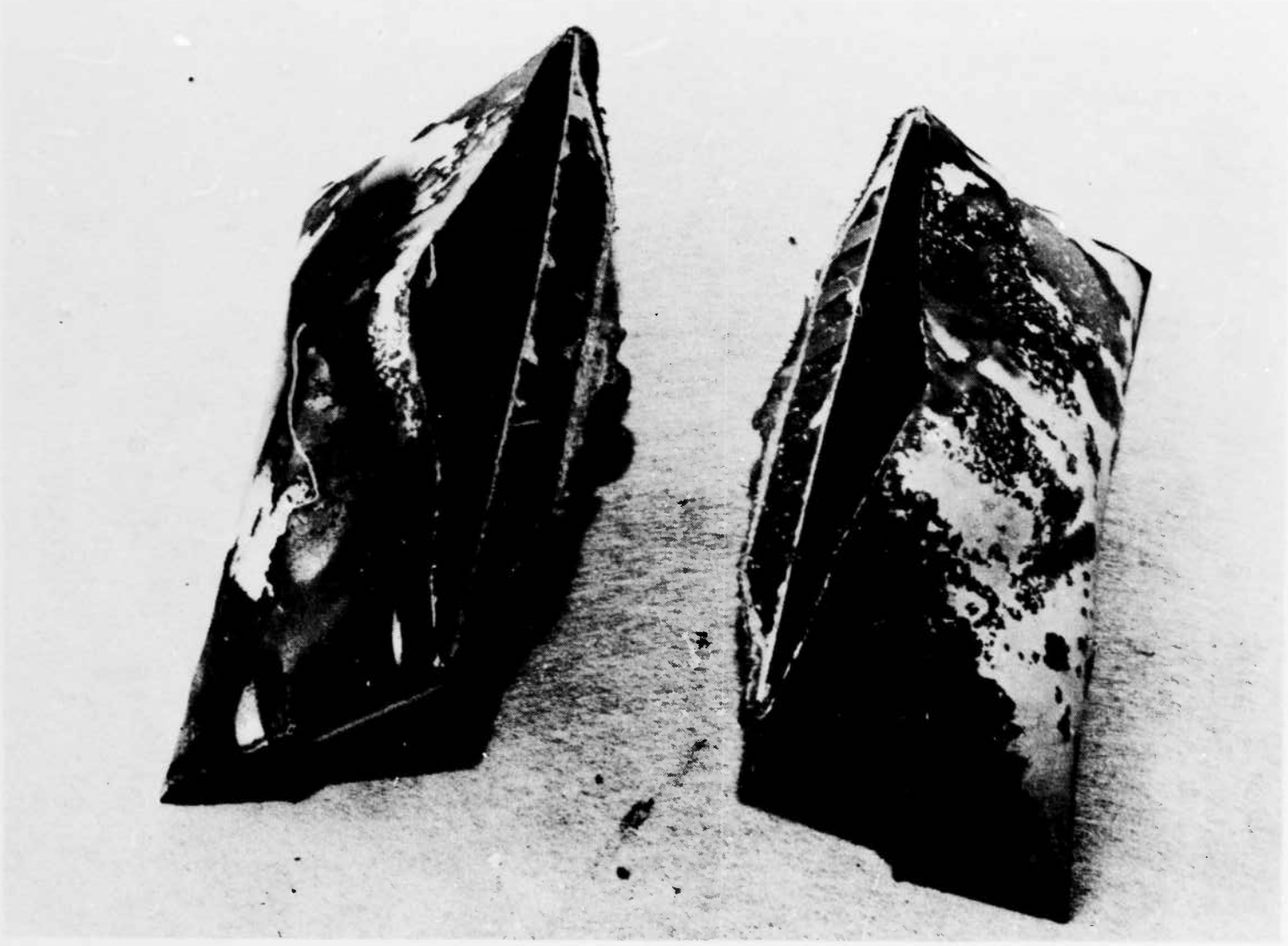

Figure 15. Panel from figure 14 cut in half for a better understanding of extent of skin buckling.

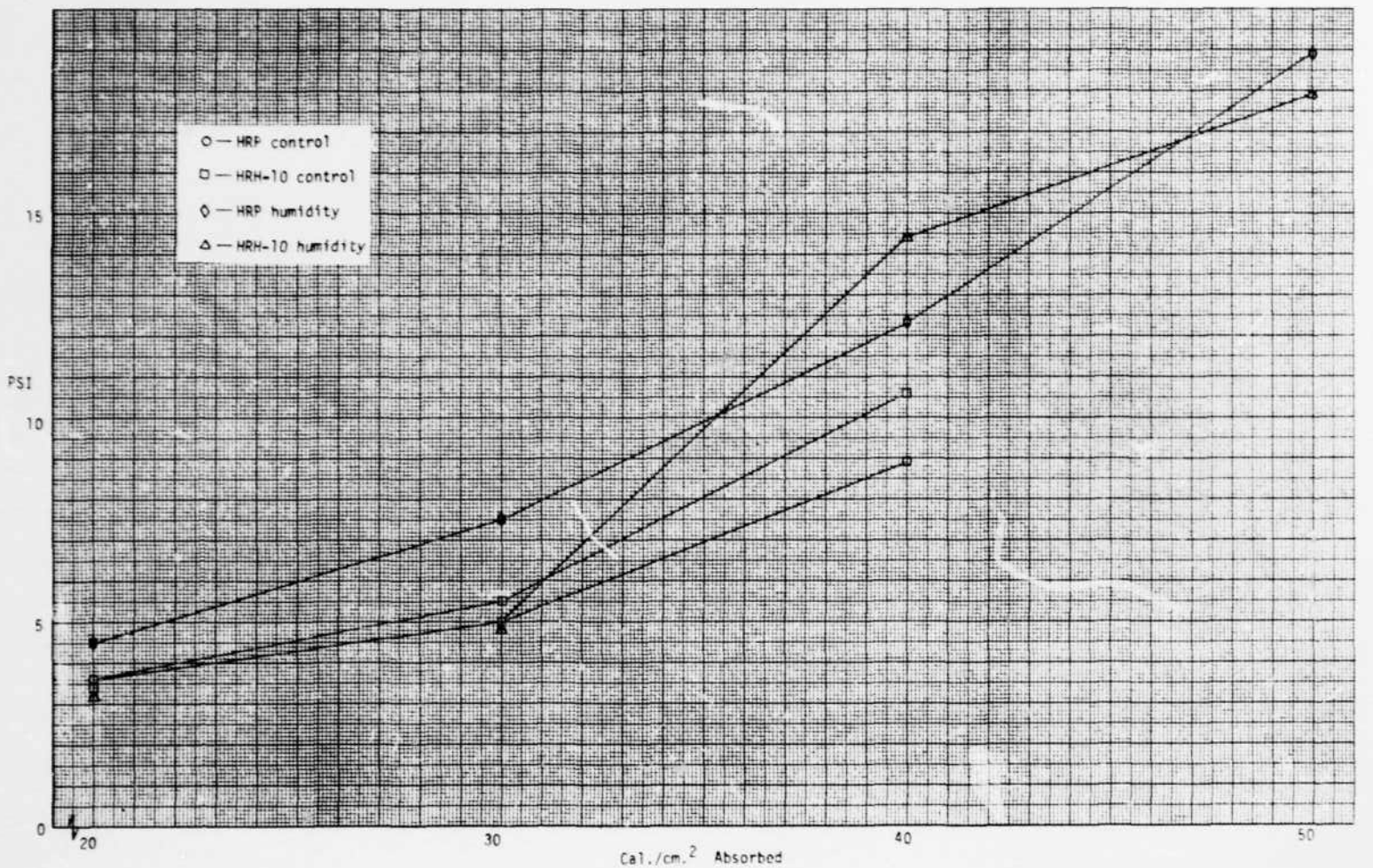

Figure 16. Humidity effects on glass-fabric epoxy honeycomb sandwich panels.

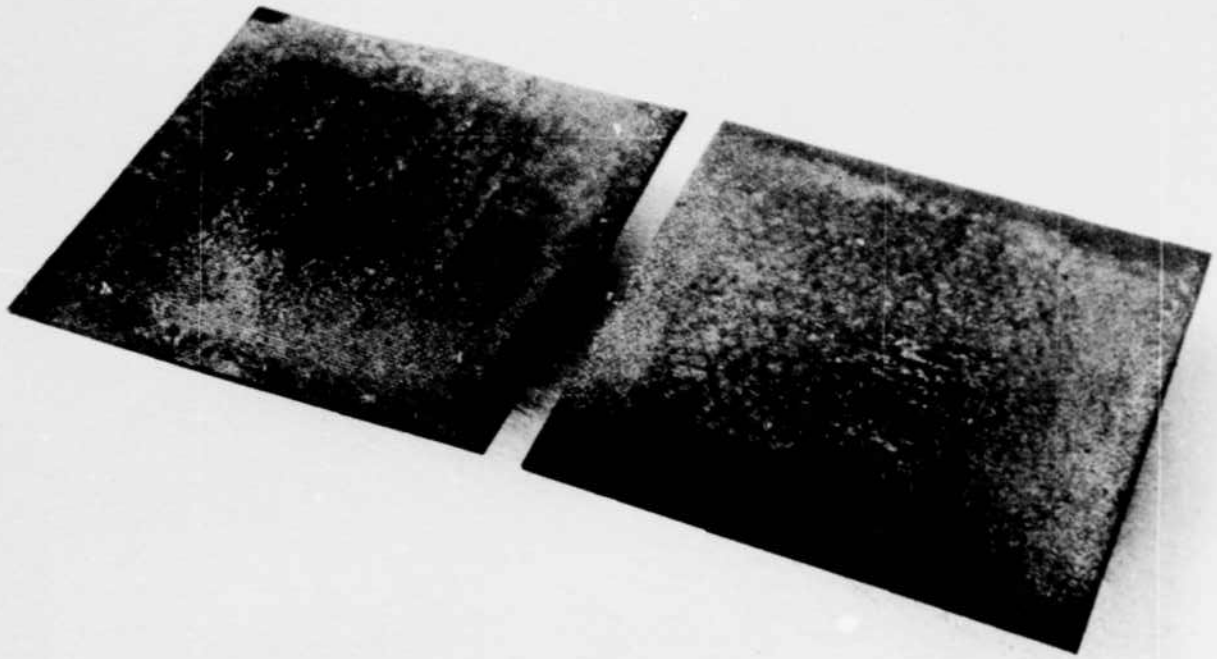

Figure 17. Control panel on right with face sheet buckling and splitting compared to humidity panel on left, both exposed to 50 cal/cm^2 absorbed.

Table 7. Humidity Data on Glass-Reinforced Epoxy Honeycomb Sandwich Panels (Made with HRP and HRH-10 cores. Values are averaged over three pulses).

Panel ID	20 cal/cm^2 Ab (psi)	30 cal/cm^2 Ab (psi)	40 cal/cm^2 Ab (psi)	50 cal/cm^2 Ab (psi)
HRP control	3.6	5.0	8.9	–
HRH-10 control	3.6	5.5	10.6	–
HRP humidity	3.6	5.0	14.4	17.9
HRH-10 humidity	4.5	7.5	12.5	18.9

NOTE: – denotes where panels would no longer hold pressure.

CONCLUSIONS

The cell pressures seen in this report as a result of thermonuclear exposure have proven to be substantial enough to cause damage to honeycomb sandwich panels. Considering the widespread use of honeycomb sandwich construction in all facets of present aircraft technology, coupled with the increasing threat from thermonuclear weapons, and the lack of design data existing in the area of cell pressure, a problem does exist. Several test panels exhibited catastrophic face sheet disbonds, while others showed severe external ply buckling which would possibly affect the aerodynamics of an aircraft. Keeping in mind the need for design data, some conclusions can be drawn from the results.

Internal cell pressure does increase with increasing levels of energy absorption. The internal cell pressure increases from one panel to the next as a function of thermal conductivity and specific heat. This is demonstrated by the following examples: metallic construction materials show higher pressures than comparable panels constructed with nonmetallic materials. Thinner panels exhibit higher temperatures resulting in higher pressures for similar thermonuclear absorption levels than do thicker panels of comparable construction.

Adhesive systems vary in their response to thermonuclear exposure. Lower temperature adhesives disbond at lower levels of absorption. Some adhesives react dramatically to thermonuclear environments as demonstrated in the tactical military aircraft panels.

Humidity saturated panels subjected to thermonuclear radiation show increases in internal pressure over identically constructed control panels. Program constraints in this area resulted in insufficient data. Although trends can be seen, firm conclusions are impossible.

Adhesive-bonded sandwich structures are used on all modern aircraft, commercial and military. Tactical and strategic military aircraft all use similar sandwich structures and are equally vulnerable to thermal degradation.

RECOMMENDATIONS

To better understand the scope of the problem of internal cell pressures as a result of thermonuclear exposure, more work is needed. Specific areas to include in future studies should be a more accurate assessment of the adhesives role in cell pressure buildup, as well as a more in-depth look into the effects of humidity. It might also be beneficial to obtain quicker response recording equipment to record those pressures which were substantial enough to blow face sheets from their native panels. Future S/V analysis of specific aircraft should contain a study of cell pressure increases utilizing the specific adhesives.

APPENDIX A

THERMAL NUCLEAR PULSE

The thermal nuclear pulse testing was performed at LAD. The thermonuclear pulse test apparatus utilizes commercially available quartz-tungsten infrared lamps. The most advanced array to date employs 29 2,000-watt bulbs stacked in an air-cooled reflector that measures 2-1/2 by 5 by 11 inches. The power to the array is controlled by a 480-volt, 450-ampere ignitron power supply. At peak power, each bulb is operated at 6,000 watts, three times their rated maximum. The power to the array is controlled, via the ignitron, by a programmable data track controller. Using this combination with the addition of a triggered shutter, precise thermal flux curves can be produced. By use of an aperature, a very uniform exposure is achieved on a 3- by 5-inch area. The peak flux obtained to date was slightly in excess of 70 calories per square centimeter per second.

The array is coupled to a 120-kw airstream to simulate in-flight effects of bursts to aircraft surfaces. Flux levels and pulse shapes are calibrated by use of copper slug calorimeters and a Barnes R4D broadband readiometer.

The thermal nuclear pulse shape used is illustrated in nondimensional form in Figure A-1.

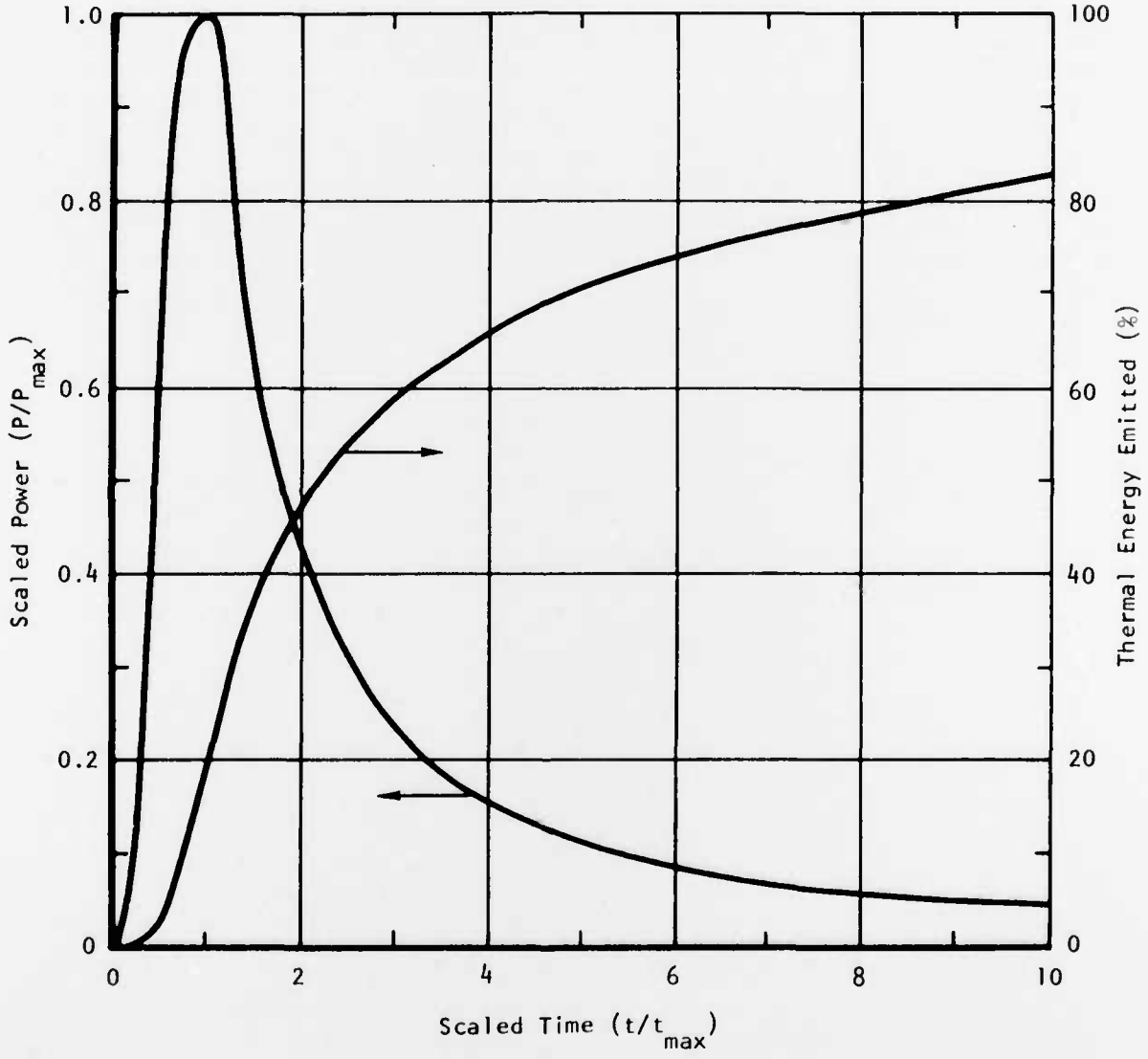

Figure A-1. Example of thermal nuclear pulse in nondimensional form.

DISTRIBUTION LIST

DEPARTMENT OF DEFENSE

Assistant to the Secretary of Defenae
Atomic Energy
ATTN: ATSD (AE)

Defense Documentation Center
Cameron Station
12 cy ATTN: TC

Defense Nuclear Agency
ATTN: STSP
ATTN: SPAS
ATTN: DDST
4 cy ATTN: TITL

Field Command
Defenae Nuclear Agency
ATTN: FCPR

Livermore Diviaion, Fld. Command, DNA
Lawrence Livermore Laboratory
ATTN: FCPRL

NATO School (SHAPE)
ATTN: U.S. Documenta Officer

Under Secretary of Def. for Rsch. & Engrg.
Department of Defenae
ATTN: Strategic & Space Syatema (OS)

DEPARTMENT OF THE ARMY

Harry Diamond Laboratoriea
Department of the Army
ATTN: DELHD-NP
ATTN: DELHD-RBH, J. Gwaltney

U.S. Army Baliiatic Reaearch Lahs.
ATTN: DRXBR-X, J. Meazaroa

U.S. Army Materiel Dev. & Readiness Cmd.
ATTN: DRCDE-D, L. Flynn

U.S. Army Nuclear & Chemical Agency
ATTN: Library

DEPARTMENT OF THE NAVY

Naval Reaearch Laboratory
ATTN: Code 2627

Naval Surface Weapona Center
ATTN: K. Candle

Naval Weapona Evaluation Facility
ATTN: P. Hughes

Strategic Syatems Project Office
Department of the Navy
ATTN: NSP-272

Office of Naval Research
ATTN: Code 464, T. Quinn

DEPARTMENT OF THE AIR FORCE

AF Materials Laboratory, AFSC
ATTN: MBC, D. Schmidt
ATTN: MBE, G. Schmitt

AF Weapons Laboratory, AFSC
ATTN: DYV, A. Sharp
ATTN: SUL

Aeroapace Syatems Division
4 cy ATTN: ENFTV, D. Ward

Foreign Technology Diviaion, AFSC
ATTN: PDBF, Mr. Spring

Strategic Air Command
Department of the Air Force
ATTN: XPFS

DEPARTMENT OF ENERGY

Sandia Laboratoriea
ATTN: Doc. Control for A. Lieber

DEPARTMENT OF DEFENSE CONTRACTORS

Aerospace Corp.
ATTN: W. Barry

Avco Reaearch & Syatems Group
ATTN: J. Patrick
ATTN: W. Broding

Boeing Co.
ATTN: E. York
ATTN: R. Dyrdahl

Boeing Wichita Co.
ATTN: D. Pierson
ATTN: R. Syring

Effecta Technology, Inc.
ATTN: R. Pariaae

General Electric Company-TEMPO
Center for Advanced Studiea
ATTN: DASIAC

Kaman AviDyne
Diviaion of Kaman Sciencea Corp.
ATTN: N. Hobba

Kaman Sciencea Corp.
ATTN: D. Sacha

Martin Marietta Corp.
Orlando Diviaion
ATTN: G. Aiello

McDonnell Douglas Corp.
ATTN: J. McCrew

Northrop Corp.
ATTN: D. Hicks

DEPARTMENT OF DEFENSE CONTRACTORS (Continued)

Prototype Development Associstes, Inc.
ATTN: J. McDonsld

R&D Associates
ATTN: A. Latter
ATTN: F. Field
ATTN: J. Csrpenter

Rockwell International Corp.
ATTN: C. Sparling
ATTN: J. Schiebler

DEPARTMENT OF DEFENSE CONTRACTORS (Continued)

Science Applicstions, Inc.
ATTN: D. Hove

SRI Internstionsl
ATTN: G. Abrshamson